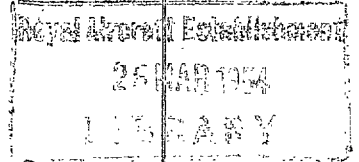




MINISTRY OF SUPPLY  
AERONAUTICAL RESEARCH COUNCIL  
REPORTS AND MEMORANDA



# Two-dimensional Aerofoil Design in Compressible Flow

*By*

L. C. Woods, M.Sc., B.E. (N.Z.), D.Phil.,  
Engineering Laboratory, Oxford University

*Crown Copyright Reserved*

LONDON : HER MAJESTY'S STATIONERY OFFICE

1953

SIX SHILLINGS NET

# Two-dimensional Aerofoil Design in Compressible Flow

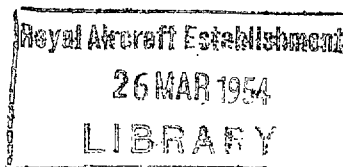
By

L. C. WOODS, M.Sc., B.E. (N.Z.), D. Phil.,  
Engineering Laboratory, Oxford University

---

*Reports and Memoranda No. 273 I*  
*November, 1949*

---



*Summary.*—This paper deals with the following two-dimensional problem:—‘The design of an aerofoil to give a specified velocity against chord curve at a given free-stream Mach number.’ A ‘relaxation’ method is adopted, based on the differential equations for incompressible and compressible flow. An essential feature of the method is that the calculations are carried out in the  $(\phi, \psi)$  or  $w$ -plane, in which the aerofoil is represented by a slit along  $\psi = 0$ . The square mesh in this plane is formed by the streamlines ( $\psi = \text{constant}$ ), and equipotentials ( $\phi = \text{constant}$ ) for incompressible flow about the aerofoil. The method is developed for a symmetrical aerofoil at zero incidence, but the modifications necessary for the more general case are indicated. A worked example is given, from which some idea of the accuracy of the method can be gained. The compressible velocity distribution about a known aerofoil was taken as the initial data. This aerofoil was actually 12 per cent thick at 30 per cent of the chord distance from the leading edge. Using a mesh giving only fourteen mesh points on the aerofoil, we find that the calculations yield a 12·06 per cent aerofoil at 28·2 per cent of the chord distance from the leading edge.

---

## *Introduction.*—*Symbols Frequently Used.*

$(x, y)$  Physical plane, in which  $z = x + iy$ .

$(\phi, \psi)$  The transformed flow plane in which the aerofoil is represented by a slit on  $\psi = 0$ .  $w = \phi + i\psi$ .

$(q_0, \theta)$  Incompressible velocity vector in polar co-ordinates.

$L_0 = \log (1/q_0)$ .

$q, L, \theta$  Similar quantities for compressible flow.

$R$  Radius of curvature of boundary.

$n$  Interval of the square mesh.

$s$  Distance along a streamline or boundary.

$X$  Residual of the Relaxation process.

$M$  Local Mach number.

$M_0$  Undisturbed stream Mach number.

$\alpha$  Angle between incompressible and compressible velocity vectors.

$q_s$  Incompressible velocity on aerofoil surface.

$a$  Local velocity of sound.

$a_0$  Velocity of sound at stagnation points.

$c$  Aerofoil chord.

$$\nabla^2 = \frac{\partial^2}{\partial \phi^2} + \frac{\partial^2}{\partial \psi^2}$$

A method of solving the incompressible flow equation  $\nabla^2 L_0 = 0$  .. .. . (1)

subject to the boundary conditions  $-\frac{\partial \theta}{\partial \phi} = \frac{\partial L_0}{\partial \psi} = \frac{1}{Rq_s}$  .. .. . (2)

and  $L_0 = \infty$  at the stagnation points, has been given in R. & M. 2726<sup>1</sup>. The difficulties encountered in the relaxation process at points neighbouring the infinities at the stagnation points for both compressible and incompressible flow are also dealt with in this reference. The compressible flow equations corresponding to (1) and (2) are developed below and we find that

$$\frac{\partial L}{\partial \psi} = \frac{\partial L_0}{\partial \psi} = \frac{1}{Rq_s} \cdot \dots \dots \dots (3)$$

If we start with given values of  $q$ , and hence  $L$ , on the aerofoil boundary, and  $L = 0$  at infinity (corresponding to an undisturbed velocity of unity) we can solve the compressible flow equations (by relaxation) and deduce the boundary gradients  $\partial L/\partial \psi$ . From (3) we then immediately have boundary conditions for the corresponding incompressible flow. The incompressible equations (1) and (2) are then solved and  $q_s$  determined. Using these values of  $(\partial L/\partial \psi)$  and  $q_s$  in (3), we can obtain  $R$  and hence deduce the aerofoil profile. A slight complication is introduced by the fact that until we know  $q_s$ , we cannot determine the positions of the equipotentials on the aerofoil surface, and until these are known we cannot assign values of  $L = L(\phi)$  on the boundary. However, proceeding from a guess for  $q_s$ , we can work through the process to find more accurate values for  $q_s$ , and so on. Convergence is quite rapid. The method is given in section 3.

Once  $\partial L/\partial \psi$  and hence  $\partial L_0/\partial \psi$  has been found, equation (1) can be solved by either (a) relaxation (R. & M. 2726<sup>1</sup>) or (b) the 'polygon method'<sup>11</sup>. Relaxation is very much slower because, although surface values only are required, the method necessitates the calculation of values throughout the whole field of flow. On the other hand the polygon method enables us to calculate surface values directly. The polygon method equation appropriate, for example, to the flow past a symmetrical aerofoil at zero incidence in a free stream is

$$\log \frac{1}{q_s}(\phi) = \frac{1}{\pi} \int_H^A \left( \frac{\partial L_0}{\partial \psi} \right) \log(\phi - \phi') d\phi' - \frac{1}{\pi} \sum_i \tau_i \log(\phi - \phi_i), \dots \dots (4)$$

where  $\tau_i$  is a discrete jump in  $\theta$  on the aerofoil surface at  $\phi = \phi_i$ .

The essential contribution of this paper is the method of deducing  $\partial L_0/\partial \psi$  from the given compressible velocity distribution.

1. *Compressible Flow*.—In Ref. 2, it is shown that

$$\frac{\partial \theta}{\partial n} - (1 - M^2) \frac{\partial L}{\partial s} = 0, \quad \text{and} \quad \frac{\partial \theta}{\partial s} + \frac{\partial L}{\partial n} = 0,$$

where  $s$  and  $n$  are distances along, and normal to the streamlines respectively. Transforming to the incompressible flow grid  $(\phi, \psi)$  we have

$$\begin{aligned} \frac{\partial}{\partial n} &= q_0 \left( \cos \alpha \frac{\partial}{\partial \psi} - \sin \alpha \frac{\partial}{\partial \phi} \right), \\ \frac{\partial}{\partial s} &= q_0 \left( \sin \alpha \frac{\partial}{\partial \psi} + \cos \alpha \frac{\partial}{\partial \phi} \right), \end{aligned}$$

where  $\alpha$  is the angle between the compressible and incompressible flow vectors.

Thus the equations assume the form

$$\frac{\partial \theta}{\partial \phi} + \frac{\partial L}{\partial \psi} = -\lambda \sin \alpha \qquad \frac{\partial \theta}{\partial \psi} - \frac{\partial L}{\partial \phi} = \lambda \cos \alpha, \dots \dots \dots (5)$$

where  $\lambda = -M^2 \left( \frac{\partial L}{\partial \phi} \cos \alpha + \frac{\partial L}{\partial \psi} \sin \alpha \right)$ .

Now, for subsonic flow at least,  $\alpha$  is quite small, and so retaining first powers of  $\alpha$  only, (5) can be written

$$\frac{\partial \theta}{\partial \psi} - \frac{\partial L}{\partial \phi} = -M^2 \left( \frac{\partial L}{\partial \phi} + \alpha \frac{\partial L}{\partial \psi} \right), \qquad \frac{\partial \theta}{\partial \phi} + \frac{\partial L}{\partial \psi} = M^2 \alpha \frac{\partial L}{\partial \phi}. \dots \dots (6)$$

Putting  $\delta = L - L_0$ , and subtracting the corresponding equations for incompressible flow, we find:—

$$\frac{\partial \alpha}{\partial \psi} - \frac{\partial \delta}{\partial \phi} = -M^2 \left( \frac{\partial L}{\partial \phi} + \alpha \frac{\partial L}{\partial \psi} \right), \qquad \frac{\partial \alpha}{\partial \phi} + \frac{\partial \delta}{\partial \psi} = M^2 \alpha \frac{\partial L}{\partial \phi}. \dots \dots (7)$$

From (6) and (7), by cross differentiating,

$$\nabla^2 \delta = \nabla^2 L = \frac{\partial}{\partial \phi} \left( M^2 \frac{\partial L}{\partial \phi} \right) + \frac{\partial}{\partial \phi} \left( M^2 \alpha \frac{\partial L}{\partial \psi} \right) + \frac{\partial}{\partial \psi} \left( M^2 \alpha \frac{\partial L}{\partial \phi} \right), \dots \dots \dots (8)$$

$$\nabla^2 \alpha = \nabla^2 \theta = \frac{\partial}{\partial \psi} \left( M^2 \frac{\partial L}{\partial \phi} \right) - \frac{\partial}{\partial \phi} \left( M^2 \alpha \frac{\partial L}{\partial \phi} \right) - \frac{\partial}{\partial \psi} \left( M^2 \alpha \frac{\partial L}{\partial \psi} \right). \dots \dots \dots (9)$$

In Appendix I more general forms of these equations are obtained, in which the vorticity is not zero. These equations find some application behind shock-waves<sup>9</sup>. The boundary condition for  $\delta$  is zero normal gradient, *c.f.* (3), while  $\alpha$  is zero on the boundaries, except at stagnation points, the location of which may change, with increase in Mach number. Equation (8) can be written with less accuracy

$$\nabla^2 \delta = \nabla^2 L = \frac{\partial}{\partial \phi} \left( M^2 \frac{\partial L}{\partial \phi} \right). \dots \dots \dots (10)$$

Now  $M^2 = \frac{q^2 M_0^2}{1 - \frac{\gamma-1}{2} M_0^2 (q^2 - 1)}$ , and  $(a_0/a)^2 = 1 + \frac{\gamma-1}{2} M^2$ ,  $\dots \dots \dots (11)$

thus  $\frac{\partial M^2}{\partial q^2} = \frac{a_0^2}{a^4}$ ; also  $q^2 = e^{-2L}$  therefore  $\frac{\partial q^2}{\partial \phi} = -2q^2 \frac{\partial L}{\partial \phi}$ .

These results enable us to write (10) in the form

$$\nabla^2 L = M^2 \left\{ \frac{\partial^2 L}{\partial \phi^2} - 2 \left( \frac{a_0}{a} \right)^2 \left( \frac{\partial L}{\partial \phi} \right)^2 \right\}. \dots \dots \dots (12)$$

Using equations (11) we can plot  $M^2$  and  $(a_0/a)^2$  as functions of  $L$ . Except for unusually thick aerofoils, and near stagnation points or sharp external corners,  $(\partial L/\partial \phi)^2$  is much smaller than  $\partial^2 L/\partial \phi^2$ , and can be neglected.  $(a_0/a)^2$  is not much larger than unity, even at large values of  $M$ , and so (12) can be written approximately:—

$$\nabla^2 \delta = \nabla^2 L = M^2 \frac{\partial^2 L}{\partial \phi^2}. \dots \dots \dots (13)$$

In the problem considered in section 5 below, results were obtained by using equation (10), *i.e.*, by ignoring  $\alpha$  completely. These results are sufficiently accurate to illustrate the method. The further step of using the full equation (8), after first using (7) to integrate through the field to find  $\alpha$ , can only be justified on a mesh of such a fineness, that the error due to the use of a *difference* equation to replace (8) is certainly smaller than that due to neglect of  $\alpha$ . However, if high accuracy is required on a fine mesh, the above remark indicates the procedure to be adopted.

2. *A Relaxation Treatment of the Equations.*—Fig. 1 is a typical square in the mesh. The value of  $L$  at point 3 say, will be indicated by  $L_3$ . Points 6 and 7 bisect the intervals (3,5) and (5,1) respectively. The mesh interval is  $n$ .

$$\text{Now} \quad n^2 \frac{\partial^2 L}{\partial \phi^2} \simeq L_1 + L_3 - 2L_5, \quad n^2 \frac{\partial^2 L}{\partial \phi^2} \simeq L_2 + L_4 - 2L_5.$$

$$\begin{aligned} \text{Therefore} \quad n^2 \nabla^2 L &\simeq \sum_{i=1}^4 L_i - 4L_5 \\ &\simeq n^2 M_5^2 \left\{ \frac{\partial^2 L}{\partial \phi^2} - 2 \left( \frac{a_0}{a} \right)^2 \left( \frac{\partial L}{\partial \phi} \right)^2 \right\}_5, \quad \text{from (12)}. \end{aligned}$$

$$\text{i.e.,} \quad \sum_{i=1}^4 L_i - 4L_5 = M_5^2 \left\{ L_1 + L_3 - 2L_5 - \frac{1}{2} \left( \frac{a_0}{a} \right)^2 (L_1 - L_3)^2 \right\},$$

$$\begin{aligned} \text{and so} \quad X_5 &= (1 - M_5^2)L_1 + L_2 + (1 - M_5^2)L_3 + L_4 - 2(2 - M_5^2)L_5 \\ &\quad + \frac{1}{2}M_5^2 \left( \frac{a_0}{a} \right)^2 (L_1 - L_3)^2 = 0, \quad \dots \dots \dots \quad (14) \end{aligned}$$

where  $X$  is termed the 'residual.' If arbitrary values of  $L$  are assigned throughout the field, in general  $X_i$ ,  $i = 1, 2, \dots$ , will not be zero. Relaxation<sup>3</sup> is the process whereby the  $X_i$  are progressively reduced to a practical minimum. While (14) is the most suitable form from which to calculate the residuals, it does not lead to a very suitable relaxation pattern.

$$\begin{aligned} \text{Now} \quad n^2 \left\{ \frac{\partial}{\partial \theta} \left( M^2 \frac{\partial L}{\partial \theta} \right) \right\}_5 &= \left( M^2 n \frac{\partial L}{\partial \theta} \right)_7 - \left( M^2 n \frac{\partial L}{\partial \theta} \right)_6 \\ &= M_7^2 (L_5 - L_3) + M_6^2 (L_5 - L_1), \end{aligned}$$

and hence equation (10), which is identical with (12), is represented by the difference equation:—

$$X_5 = (1 - M_7^2)L_1 + L_2 + (1 - M_6^2)L_3 + L_4 - \{4 - (M_7^2 + M_6^2)\}L_5 = 0,$$

from which we find the 'influence coefficients'

$$\frac{\partial X_5}{\partial L_{2,4}} = 1, \quad \frac{\partial X_5}{\partial L_5} = 4 - (M_6^2 + M_7^2), \quad \frac{\partial X_5}{\partial L_1} = 1 - M_7^2, \quad \frac{\partial X_5}{\partial L_3} = 1 - M_6^2. \quad \dots \quad (15)$$

These give rise to the relaxation pattern shown in Fig. 2.  $M^2$  and  $\frac{1}{2}(a_0/a)^2$  are readily determined from a graph, in which they are plotted as functions of  $L$ . It is sufficient to estimate  $L_6$  and  $L_7$  to obtain values of  $M_6^2$  and  $M_7^2$ . The small errors introduced in this way are detected when (14) is used to recompute the residuals towards the end of the relaxation.

On the aerofoil boundary (14) and (15) are modified as follows. Referring to Fig. 1, in which the line 153 is now taken to represent an aerofoil boundary, we have from (3)

$$2n \left( \frac{\partial L}{\partial \psi} \right)_5 = \left( \frac{2n}{Rq_s} \right)_5 = L_2 - L_4,$$





(v) Equation (16), in which of course  $X_5 = 0$ , is now used to determine  $(\partial L/\partial \psi) = f(\phi)$ , (22) and this by (3) is the normal boundary gradient for the corresponding incompressible flow.

(vi) Using this aerofoil boundary condition, with appropriate outer boundary conditions, we now solve the incompressible-flow equation (1) to obtain a new and more accurate value of  $q_s = q_s(\phi)$ . . . . . (23)

Integration of  $ds = d\phi/q_s(\phi)$  yields  $s = s(\phi)$ . (See Appendix for formula to use when this integrand becomes infinite at the stagnation points.)

(vii) From (2),  $d\theta = -(\partial L/\partial \psi) d\phi = d\theta(\phi)$ , and so with  $\theta(0) = \tau_H$ , and  $(\partial L/\partial \psi)$  given by (22), we can integrate to find  $\theta(\phi)$ . Then  $dx = ds \cos \theta$ ,  $dy = ds \sin \theta$ , are integrated to give  $x = x(\phi)$ ,  $y = y(\phi)$ ,  $c = x(10)$ , which parametrically define the aerofoil profile. The process is set out for the selected example in Table 3.

Since in step (vi) we obtained  $q_s(\phi)$ ,  $s(\phi)$ , we can deduce  $q_s = q_s(s)$ . Using the value of  $c$  found in step (vii), we find a new value of  $q_s = q_s(s/c)$  to use in step (ii). We repeat steps (ii) to (vii) until there is negligible difference between successive values of  $q_s(s)$ . The final relations  $x(\phi)$ ,  $y(\phi)$  found this way then define the aerofoil profile.

The process may appear to be very laborious, but when steps (i) to (vii) have been worked through once, only a fraction of the time is required to repeat them. Convergence is rapid, and the process needs to be repeated only two or three times.

#### 5. Modifications Necessary for an Asymmetric Aerofoil.—Only two modifications are necessary.

(a) Using an approximate  $q_s$  calculated, not from (20), but from the corresponding von Kármán equation for flow with circulation<sup>8</sup>, we find an approximate circulation  $K = \oint q_s d(s/c) = \Delta\phi$ , where  $\Delta\phi$  is the potential jump at the front stagnation point, taking  $\phi = 0$  at the trailing edge. Thus on the upper surface  $\phi$  varies from 0 to 10 say, while on the lower surface  $\phi$  varies from 0 to 10 —  $\Delta\phi$ . Integrations are now necessary on both upper and lower surfaces, and the upper limits of these integrations are different.

(b) The circulation makes a substantial contribution to the substitution vortex calculated for the outer boundary in the open field.

6. An Example: A Symmetrical Aerofoil in a Channel.—In Ref. 7 Emmons started with a symmetrical aerofoil of specified profile between channel walls, and deduced the velocity distribution curve for flow at several Mach numbers. He used an entirely different approach to that given above, based on the compressible-flow stream function. He gives experimental curves agreeing closely with his theoretical results. For these reasons this has been selected as a suitable example to illustrate the method of this paper. We shall start with his  $q = q(x/c)$ -curve at  $M = 0.70$ , and deduce the aerofoil profile, which can then be compared with the actual profile.

Table 1.—This sets out  $q(x/c)$  at  $M = 0.70$ , the deduced  $q_s(x/c)$  using equation (20), and for comparison, the value of  $q_s(x/c)$  given by Emmons.

Table 2 gives the true aerofoil coordinates, while Fig. 4 gives the geometric relationship between the aerofoil and channel. Of course at the start of the problem we are only supposed to know that  $H/c = 3.6$ .

Applying equation (21) we find a first approximation to  $c$ . This is  $c = 9.26$ . If  $\psi = 0$  on the axis, and  $\psi'$  is the value of  $\psi$  on the upper channel wall, then far upstream, where  $q = 1$ ,  $2\psi'/H = q = 1$ . Therefore  $\psi' = H/2$ , but  $H/c = 3.6$ , and so

$$\psi' = \frac{3.6 \times 9.26}{2} = 16.65 \approx 17,$$

say, as an initial approximation. We can now set up the square mesh in the  $w$ -plane. Fig. 5 shows a part of the grid actually used in the relaxation. Using the last three entries in Table 1, column 3, we find that an estimate for the value of  $\tau$  is 8.55 deg.

Table 3 sets out steps (vi) and (vii) of section 4, for the third and in this case, final round of the process outlined in that section. We shall describe the columns of the table that are not obvious.

Column 2 Values of  $q_s$  from the previous round.

Column 4  $\delta s = \frac{\delta\phi}{q_s}$  (Use formula (30) of Appendix II for the first and last steps).

Column 5  $\delta\theta = \left(\frac{\partial L}{\partial\psi} \delta\theta\right)$  expressed in degrees.

$\delta\theta_m$  mean value of  $\delta\theta$  at midpoints of the intervals of  $\phi$ .

Column 8  $\delta s - \delta x = \delta s(1 - \cos\theta)$

Column 9  $x$  from columns (8) and (4).  $c$  is the value of  $x$  at  $\phi = 10$ .

Column 11  $\delta y = \delta s \sin\theta$ .

The results given in columns 10 and 12 are shown plotted in Fig. 6, and can be compared with the actual aerofoil profile also shown in the Figure. The values of  $q$ ,  $q_s$  given in Table 1 and in Column 2 above, are graphed in Fig. 7.

Now with  $\psi' = 17$ ,  $c = 9.110$ , we have  $H/c = \frac{2 \times 17}{9.110} = 3.73$ , instead of 3.6 as specified.

The next step is to change the mesh so that  $\psi' = (3.6 \times 9.110)/2 \approx 16.5$ . This means that interpolation formulae are required when relaxing on or adjacent to the channel walls. However, making this change, we find that the new residuals are such to make a negligible contribution to  $q_s$ .

It will be noticed in Table 3 that  $y$  at  $\phi = 10$  is not zero as it should be. This is, of course, due to the coarse mesh used in the neighbourhood of the nose. With a fine mesh, instead of relying on the value of the trailing-edge angle, calculated from (19) we could arrange this angle so that  $y$  is zero at the nose. The fine mesh, however, means a great deal more computation.

In this case there is another check. Integrating  $d\theta = \frac{\partial L}{\partial\psi} d\psi$  from the channel wall, where  $\theta = 0$ , along  $\phi = 6$  we find  $\theta = 1.66$  on the aerofoil, which is sufficiently close to the value of 1.63 obtained in Table 3.

6. *Conclusions.*—Considering the sources of error, which are:—

(a) due to using a finite difference equation instead of the differential equation,

(b) due to neglect of  $\alpha$ ,

(c) possible small errors in the results taken from Emmons' paper (Emmons provided graphs only),

the comparison between the results of this method and those given by Emmons, given in Figs. 5 and 6, is quite good. The method would thus appear to be a suitable one for the design of aerofoils in compressible flow. Problems in which the profile is given, and the velocity field is required, have been solved along similar lines (R. & M. 2727<sup>10</sup>. See also Appendix III). The method is quite satisfactory for small supersonic patches on the aerofoil, and presumably the design problem could also be solved if the specified velocity distribution has a small supersonic section.

7. *Acknowledgements.*—The compressible-flow equations given in section 1, and in the appendix, were brought to the author's attention, in a different form, by Professor Thom, who has used these equations in a somewhat different method<sup>6</sup> to that given in section 2, to solve compressible-flow problems.

## REFERENCES

No.	Author	Title, etc.
1	L. C. Woods .. ..	The Arithmetical Solution of Two-dimensional Partial Differential Equations in the Neighbourhood of a Stagnation Point or Boundary Discontinuity. R. & M. 2726. October, 1949.
2	Liepmann and Puckett .. ..	<i>Introduction to Aerodynamics of a Compressible Fluid.</i> Wiley & Sons, 1947.
3	R. V. Southwell .. ..	<i>Relaxation Methods in Theoretical Physics.</i> Oxford University Press. 1946.
4	L. M. Milne-Thomson .. ..	<i>Theoretical Aerodynamics.</i> Macmillan and Co. 1948.
5	A. Thom .. ..	Blockage Corrections in a Closed High-Speed Tunnel. R. & M. 2033. November, 1943.
6	A. Thom and L. Klanfer .. ..	Compressible Flow past an Aerofoil. A.R.C. 12,476. (Unpublished.)
7	H. Emmons .. ..	Flow of a Compressible Fluid past a Symmetrical Airfoil in a Wind Tunnel and in Free Air. N.A.C.A. Tech. Note 1746. November, 1948.
8	Lin .. ..	On an Extension of the von Kármán-Tsien Method to Two-dimensional Subsonic Flows with Circulation around Closed Profiles. <i>Quart. Journ. Appl. Maths.</i> , vol. IV, No. 3. 1946.
9	L. C. Woods .. ..	A Relaxation Treatment of Shock Waves. A.R.C. 13,242. July, 1950. (Unpublished.)
10	L. C. Woods and A. Thom .. ..	A new Relaxational Treatment of the Compressible Two-dimensional Flow about an Aerofoil with Circulation. R. & M. 2727. March, 1950.
11	L. C. Woods .. ..	Incompressible Two-dimensional Flow of an Inviscid Fluid about a Symmetrical Aerofoil in a Channel or Free Stream. A.R.C. 13,240.
12	M. J. Lighthill .. ..	A New Method of Two-dimensional Aerodynamic Design. R. & M. 2112. April, 1945.
13	Shen Yuan .. ..	A Theoretical Investigation of Compressible Flow around Cylinders at Large Mach Numbers. A.R.C. 8,254. 1944.
14	I. Imai and T. Aihara .. ..	On the Subsonic Flow of a Compressible Fluid past an Elliptic Cylinder. Tokyo Report No. 194. A.R.C. 5,658. August, 1940.

---

## APPENDIX I

To prove:—

$$\nabla^2 L = - \frac{\partial}{\partial \phi} \left( \lambda \cos \alpha + \frac{\zeta}{q_0 q} \sin \alpha \right) - \frac{\partial}{\partial \psi} \left( \lambda \sin \alpha - \frac{\zeta}{q_0 q} \cos \alpha \right),$$

$$\nabla^2 \alpha = - \frac{\partial}{\partial \phi} \left( \lambda \sin \alpha - \frac{\zeta}{q_0 q} \cos \alpha \right) + \frac{\partial}{\partial \psi} \left( \lambda \cos \alpha + \frac{\zeta}{q_0 q} \sin \alpha \right),$$

where  $\lambda = -M^2 \left( \cos \alpha \frac{\partial L}{\partial \phi} + \sin \alpha \frac{\partial L}{\partial \psi} \right)$ ,  $L = \log(1/q)$ , and  $\zeta$  is the vorticity.

*Proof.*—We shall denote by  $\text{Re } a$ , the real part of  $a$ , and by  $\text{Im } a$ , the imaginary part of  $a$ .  $\rho$  is the density.

1. *Continuity*.—This equation can be written

$$\frac{\partial}{\partial x} (\rho q \cos \theta) + \frac{\partial}{\partial y} (\rho q \sin \theta) = 0.$$

or  $\text{Rl } 2 \frac{d}{dz} (\rho q e^{i\theta}) = 0,$

since  $2 \frac{d}{dz} = \frac{\partial}{\partial x} - i \frac{\partial}{\partial y},$  and thus

$$\text{Rl} \left( \frac{\partial}{\partial x} - i \frac{\partial}{\partial y} \right) \rho q (\cos \theta + i \sin \theta) = \frac{\partial}{\partial x} (\rho q \cos \theta) + \frac{\partial}{\partial y} (\rho q \sin \theta).$$

Transforming to the  $w$ -plane, we have for the velocity vector;

$$q_w = q_z \frac{dz}{dw}, \text{ i.e., } q_w = q_z/q_0, \text{ also } \theta_w = \theta_z - \theta_0 = \alpha.$$

Therefore in the  $w$ -plane continuity can be written

$$\text{Rl } 2 \frac{d}{dw} \left( \rho \frac{q}{q_0} e^{i\alpha} \right) = 0. \quad \dots \dots \dots \quad (24)$$

2. *Vorticity*.— $\text{Im} \left( \frac{\partial}{\partial x} - i \frac{\partial}{\partial y} \right) q (\cos \theta + i \sin \theta) = \left( \frac{\partial}{\partial x} (q \sin \theta) - \frac{\partial}{\partial y} (q \cos \theta) \right) = \zeta,$

and hence the equation can be written  $\text{Im } 2 \frac{d}{dz} (q e^{i\theta}) = \zeta.$

In the  $w$ -plan this becomes  $\text{Im } 2 \frac{d}{dw} \left( \frac{q}{q_0} e^{i\alpha} \right) = \zeta/q_0^2. \quad \dots \dots \dots \quad (25)$

3. *Bernoulli's equation* is:—

$$q \frac{dq}{ds} = - \frac{a^2}{\rho} \frac{d\rho}{ds}, \text{ i.e., } M^2 \frac{dL}{ds} = \frac{1}{\rho} \frac{d\rho}{ds}. \quad \dots \dots \dots \quad (26)$$

Since  $\frac{d}{ds} = \cos \alpha \frac{\partial}{\partial \phi} + \sin \alpha \frac{\partial}{\partial \psi},$  we can write (26) in the form

$$M^2 \text{Rl} \left( e^{i\alpha} \frac{dL}{dw} \right) = \frac{1}{\rho} \text{Rl} \left( e^{i\alpha} \frac{d\rho}{dw} \right) = - \lambda/2. \quad \dots \dots \dots \quad (27)$$

Now from equation (24)  $\text{Rl} \left\{ \rho \frac{d}{dw} \left( \frac{q}{q_0} e^{i\alpha} \right) + \frac{q}{q_0} e^{i\alpha} \frac{d\rho}{dw} \right\} = 0.$

Therefore  $e^{-i\alpha} \frac{q_0}{q} \text{Rl} \frac{d}{dw} \left( \frac{q}{q_0} e^{i\alpha} \right) + \frac{1}{\rho} e^{-i\alpha} \text{Rl} \left( e^{i\alpha} \frac{d\rho}{dw} \right) = 0.$

With the aid of (25) and (27) this equation becomes

$$2e^{-i\alpha} \frac{q_0}{q} \frac{d}{dw} \left( \frac{q}{q_0} e^{i\alpha} \right) = e^{-i\alpha} \left( \lambda + i \frac{\zeta}{q_0 q} \right).$$

Therefore  $4 \frac{d^*}{dw} \frac{d}{dw} \left( \log \frac{q}{q_0} e^{ia} \right) = 2 \frac{d^*}{dw} \left[ e^{-ia} \left( \lambda + i \frac{\zeta}{q_0 q} \right) \right],$

where  $2 \frac{d^*}{dw} = \frac{\partial}{\partial \phi} + i \frac{\partial}{\partial \psi}$

i.e.,  $\nabla^2 \log \frac{q}{q_0} e^{ia} = 2 \frac{d^*}{dw} \left\{ e^{-ia} \left( \lambda + i \frac{\zeta}{q_0 q} \right) \right\}, \dots \dots \dots (28)$

whereas for incompressible flow  $\nabla^2 \log q_0 = 0. \dots \dots \dots (29)$

The real and imaginary parts of (28), with the aid of equation (29), yield the equations required to be proved.

---

## APPENDIX II

### *Formula at Stagnation Points.*

In R. & M. 2726<sup>1</sup> the formula

$$s = \int_0^s \frac{d\phi}{q} = \frac{1}{(1 - \tau/2\pi)} \frac{\phi'}{q'} \dots \dots \dots (30)$$

is established for the value of  $s$  measured from a stagnation point of trailing-edge angle of  $\tau$ , to the point on the aerofoil at which  $\phi = \phi', q = q'$ .

---

## APPENDIX III

This Appendix contains the results of an investigation into the compressible flow about a circular cylinder by the method outlined in sections 1 and 2. Results are obtained at values of  $M_0$  of 0.35, 0.40 and 0.45. The most interesting feature of the solutions is that at the higher Mach numbers the velocity peak moves off to one side of its usual symmetrical position on a circular cylinder.

This relatively simple profile was actually selected as a preliminary example to ensure that no special difficulties had been overlooked, but in any case so much work has been done on the circular cylinder by various investigators that the results obtained here have an intrinsic value.

The incompressible solution could have been entirely calculated by theory, but relaxation was used so that the approximate theory of R. & M. 2726 could be applied, and hence its accuracy checked by comparison with exact theory.

*Incompressible Flow.*—Suppose the cylinder of radius  $a$  is situated at the origin, then if the velocity at infinity is unity and parallel to the real axis, the  $(\phi, \psi)$  and  $(x, y)$ -planes are related by

$$w = \phi + i\psi = - \left( z + \frac{a^2}{z} \right), \text{ where } z = x + iy$$

or writing  $z = re^{i(\pi/2-\alpha)}$ ,

$$\phi = -r \sin \alpha \left(1 + \frac{a^2}{r^2}\right), \quad \psi = -r \cos \alpha \left(1 - \frac{a^2}{r^2}\right). \quad (31)$$

The velocity is given by  $qe^{i\theta} = \frac{dw}{dz} = 1 - \frac{a^2}{z^2}$ ,

$$i.e., \quad q = \left\{1 + 2 \left(\frac{a}{r}\right)^2 \cos 2\alpha + \left(\frac{a}{r}\right)^4\right\}^{1/2}, \quad \tan \theta = -\frac{\sin 2\alpha}{\cos 2\alpha + \left(\frac{r}{a}\right)^2}. \quad (32)$$

Writing  $p = (a/r)^2$ , we find from (31) the reciprocal quartic

$$a^2 \left(p^2 + \frac{1}{p^2}\right) - (\phi^2 + \psi^2) \left(p + \frac{1}{p}\right) + 2(\phi^2 - \psi^2 - a^2) = 0, \quad (\text{since } p \neq 0).$$

Writing  $p + 1/p = t$ , say, reduces this equation for  $p$  to two quadratics, which are easily solved.

From (32) it follows that

$$q = \frac{1}{1+p} \left\{(1+p)^4 - \frac{4p^2}{a^2} \phi^2\right\}^{1/2}, \quad \tan \theta = \frac{-2\psi\phi p(1+p)^2}{(1-p^2)\{a^2(1+p)^3 - 2p\phi^2\}}$$

This method enables  $q$  and  $\theta$  to be found at specified values of the ratios  $\phi/a$ ,  $\psi/a$ , but it can be seen that even for this simple problem the theoretical solution in the  $(\phi, \psi)$ -plane is not easy (from the computational point of view) to obtain. In fact it was quicker to use relaxation in the main part of the field. The theoretical solution was used to calculate results in the neighbourhood of the stagnation point and thus to check the approximate theory of R. & M. 2726, which was justified by the results. Boundary values on the cylinder and on an outer boundary at a large distance from the cylinder were also calculated by the exact theory. Fig. 9 shows a portion of the  $(\phi, \psi)$ -mesh on which the relaxation was carried out.

*Compressible Flow.*—The only change in the calculations from the design method was in the use of equation (16) to calculate  $X_s$  instead of using it to calculate values of the gradient, which are now known. No special difficulties occurred in calculating the compressible flow. The angle between the compressible and incompressible-flow vectors was ignored and, as a check on this approximation, this angle was calculated for  $M_0 = 0.35$ , for which its maximum value in the field was less than 2 deg. The results for  $M_0 = 0.35, 0.40$  and  $0.45$  are shown in Figs. 8, 10, 11 and 12.

Shen Yuan<sup>13</sup> found results similar to those of Fig. 8 by an application of the hodograph transformation. At the higher Mach numbers the velocity peak moved off to one side of its usual symmetric position on a circular cylinder. Yuan's results are not strictly comparable with the author's, since, as  $M_0$  increased, his cylinder distorted in shape. This profile distortion is an undesirable feature associated with the hodograph method.

The results in Fig. 8 indicate that the lower critical Mach number ( $M_c$ ) is slightly less than 0.4 whereas the Janzen-Rayleigh<sup>14</sup> method gives  $M_c = 0.42$ . Without a recalculation on a finer mesh the author cannot be confident that  $M_c > 0.4$ , but the error in calculation from this source would not account for a discrepancy of 0.2 in  $M_c$ .

The author was unable to find a continuous solution at  $M_0 = 0.50$ . This was to be expected since it is known that the Mach number at which shock-waves appear for a cylinder is about  $M_0 = 0.475$ . In the relaxation the residuals could not be eliminated, and it was concluded that this indicated the need to introduce a shock-wave into the field.

TABLE 1

*Surface Velocities*

(1) $x/c$ %	(2) $q$ ( $M = 0.7$ )	(3) $q_0$ (v. Kármán)	(4) $q_0$ (Emmons)
1	0.905	0.925	0.920
1.8	1.060	1.046	—
3	1.159	1.104	1.123
4	1.197	1.127	1.149
6	1.252	1.156	1.170
8	1.274	1.168	1.178
10	1.296	1.180	1.183
12	1.307	1.185	1.188
14	1.320	1.193	1.188
16	1.332	1.197	1.188
18	1.338	1.200	1.188
20	1.340	1.201	1.183
24	1.317	1.192	1.175
26	1.303	1.183	1.169
30	1.276	1.169	1.155
40	1.228	1.143	1.132
50	1.187	1.120	1.107
60	1.135	1.089	1.083
70	1.095	1.064	1.058
80	1.039	1.029	1.023
90	0.990	0.992	0.990
95	0.948	0.960	0.955

TABLE 2

*True Aerofoil Co-ordinates*

$x/c$ %	$y/c$ %
0	0
1.25	1.894
2.5	2.615
5.0	3.555
7.5	4.200
10	4.683
15	5.345
20	5.738
25	5.941
30	6.002
40	5.803
50	5.294
60	4.563
70	3.664
80	2.623
90	1.448
95	0.807
100	0

L.E. Radius =  $1.58\%c$ .

TABLE 3

*Determination of Profile Co-ordinates*

(1)	(2)	(3)	(4)	(5)	(5)	(6)	(7)	(8)	(9)	(10)	(11)	(12)	
$\phi$	$\delta\phi$	$q$	$1/q$	$\delta s$	$\delta\theta$	$\delta\theta_m$	$\theta$	$\theta_m$	$(\delta s - \delta x) \times 10^3$	$x$	$x/c\%$	$\delta y \times 10^2$	$y/c\%$
0		0.000	—	—		—		—		—	—		—
1	1	0.995	1.005	1.048	1.02	1.32	7.23	7.89	11	1.037	11.4	145	1.57
2	1	1.033	0.968	0.987	0.61	0.82	6.41	6.82	7	2.017	22.2	117	2.86
3	1	1.069	0.936	0.952	1.08	0.85	5.56	5.96	5	2.964	32.6	99	3.94
4	1	1.094	0.914	0.925	1.14	1.11	4.46	5.01	4	3.885	42.7	81	4.83
5	1	1.119	0.894	0.904	1.37	1.26	3.19	3.82	2	4.787	52.7	60	5.49
6	1	1.139	0.878	0.885	1.65	1.56	1.63	2.61	1	5.671	62.4	40	5.92
7	1	1.156	0.865	0.871	2.44	2.05	— 0.42	0.60	0	6.542	71.8	9	6.03
7 $\frac{1}{2}$	$\frac{1}{2}$	1.170	0.855	0.430	1.52	1.37	— 1.79	— 1.11	0	6.972	76.7	— 8	5.94
8	$\frac{1}{2}$	1.178	0.850	0.426	2.09	1.81	— 3.60	— 2.70	0	7.398	81.3	— 20	5.72
8 $\frac{1}{2}$	$\frac{1}{2}$	1.182	0.845	0.424	2.32	2.21	— 5.81	— 4.71	2	7.831	86.0	— 35	5.34
9	$\frac{1}{2}$	1.180	0.848	0.423	3.63	2.98	— 8.79	— 7.30	3	8.241	90.6	— 54	4.73
9 $\frac{1}{4}$	$\frac{1}{4}$	1.177	0.850	0.212	2.74	3.19	— 12.08	— 10.38	3	8.450	92.8	— 38	4.32
9 $\frac{1}{2}$	$\frac{1}{4}$	1.167	0.857	0.213	4.96	3.85	— 15.73	— 13.91	6	8.657	95.2	— 51	3.76
9 $\frac{3}{4}$	$\frac{1}{4}$	1.105	0.905	0.220	8.38	6.67	— 22.50	— 19.17	13	8.864	97.4	— 72	2.97
10	$\frac{1}{4}$	0.000		0.279	—	10.67	—	— 27.83	33	9.110	100.0	— 131	1.66

All distances measured from the trailing edge.

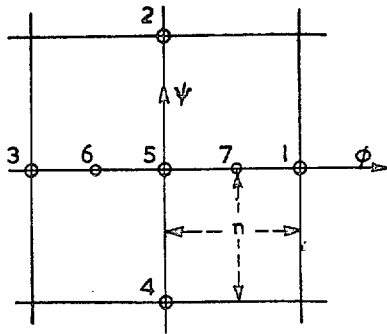


FIG. 1.

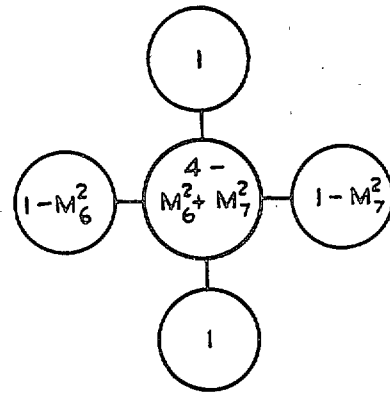


FIG. 2. Relaxation Pattern.

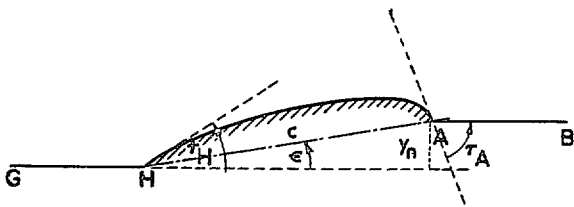


FIG. 3.

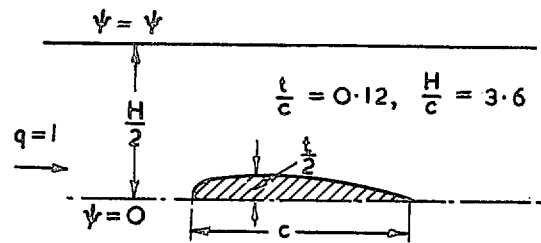


FIG. 4.

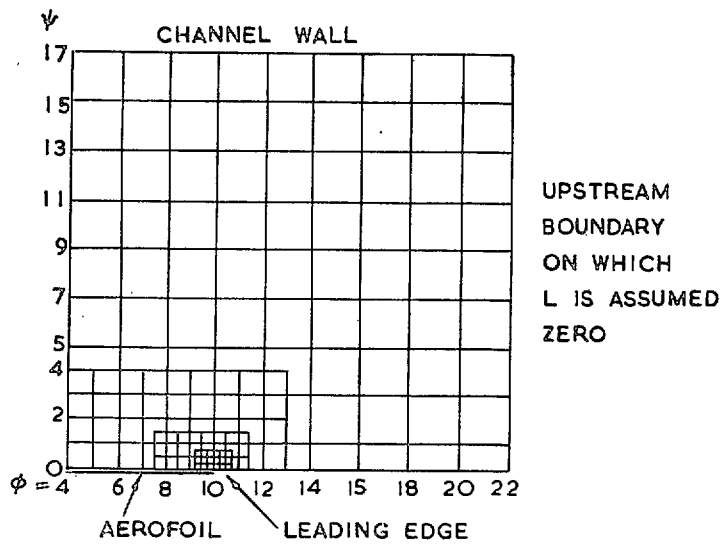


FIG. 5. Section of relaxation mesh.

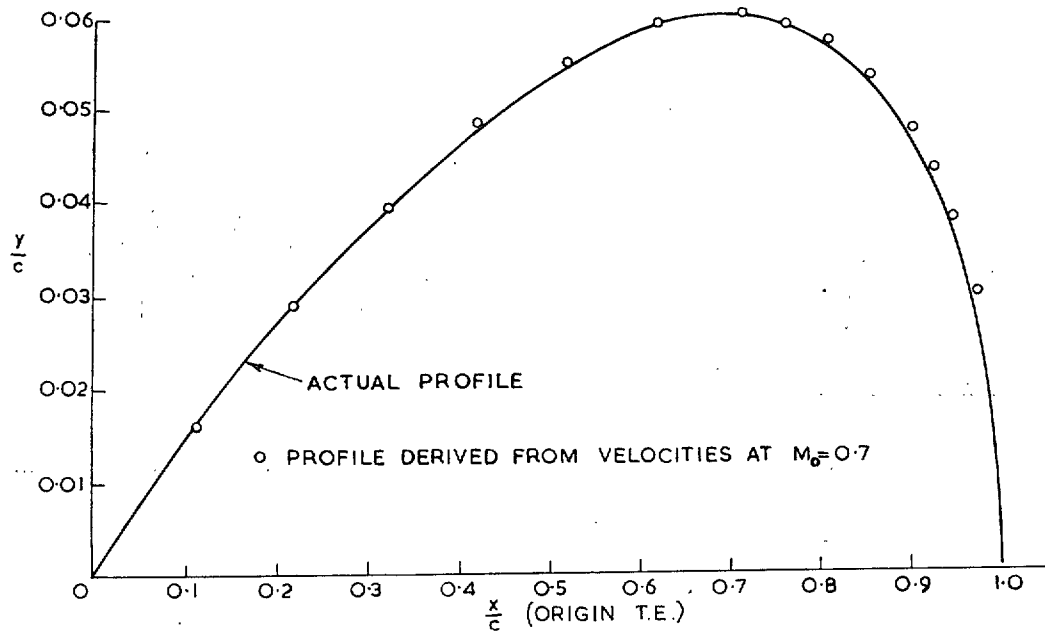


FIG. 6. Aerofoil profile; actual and deduced.

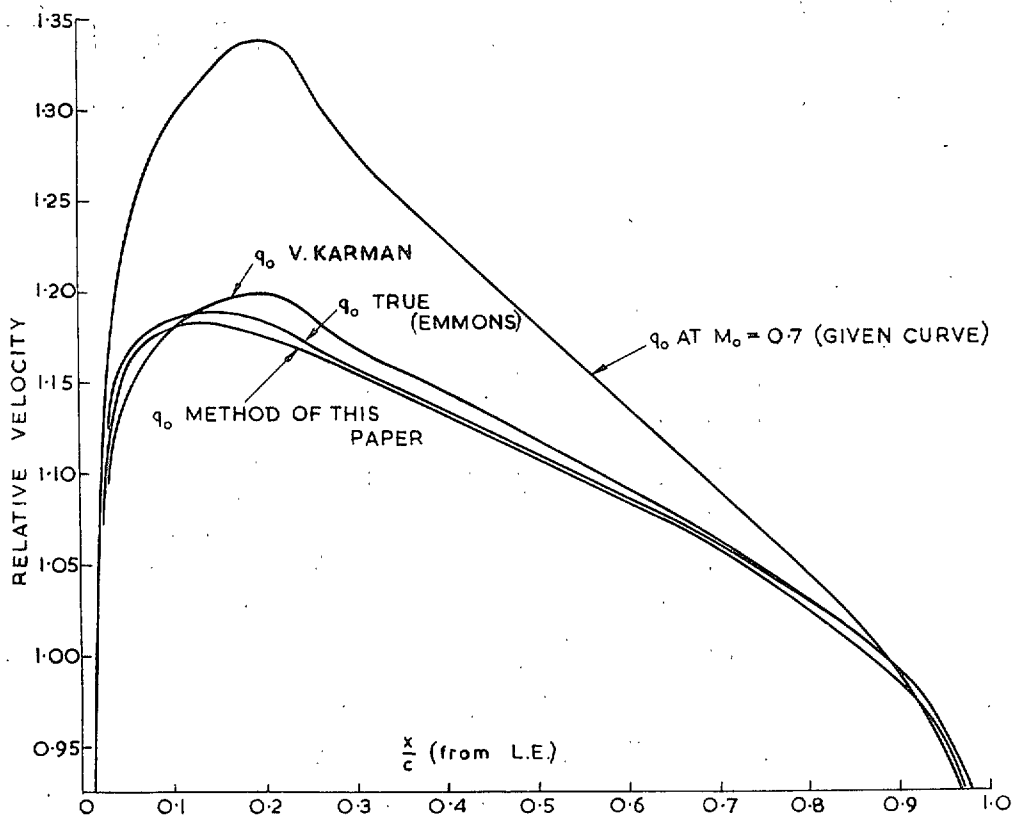


FIG. 7. Velocity distributions.

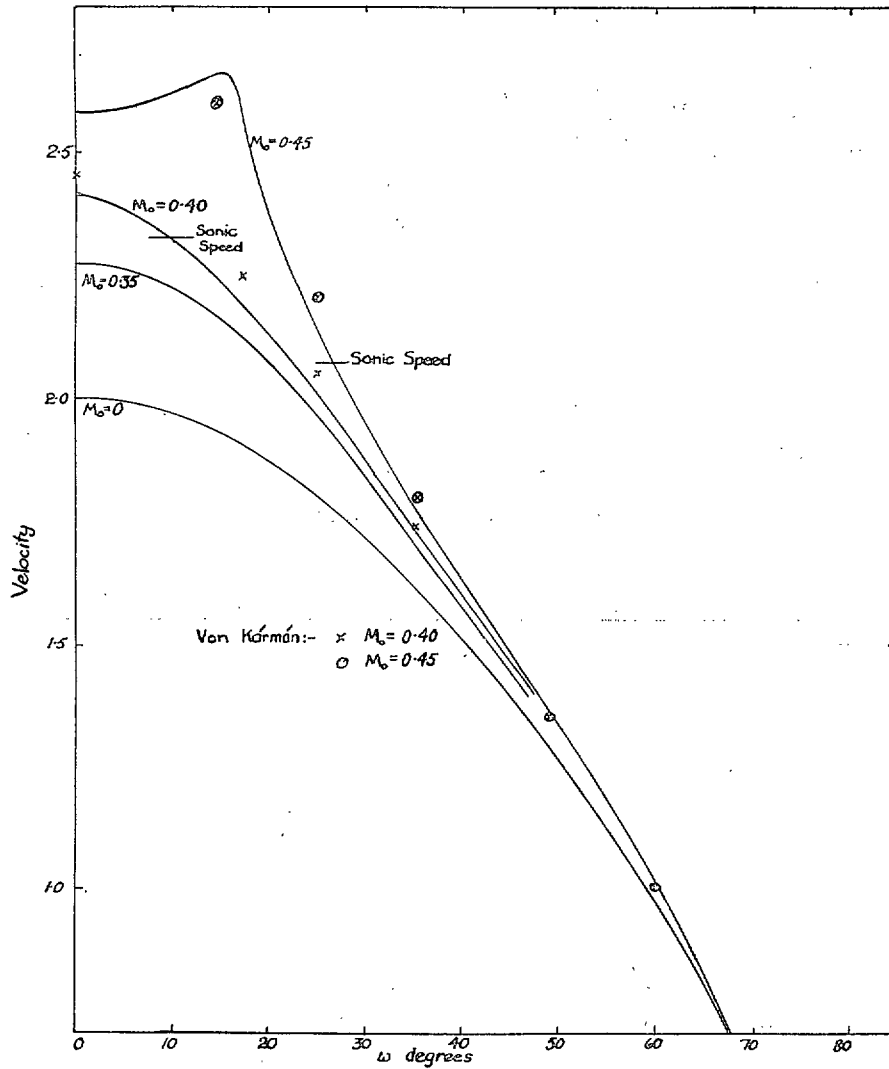


FIG. 8. Velocity distribution for cylinder.

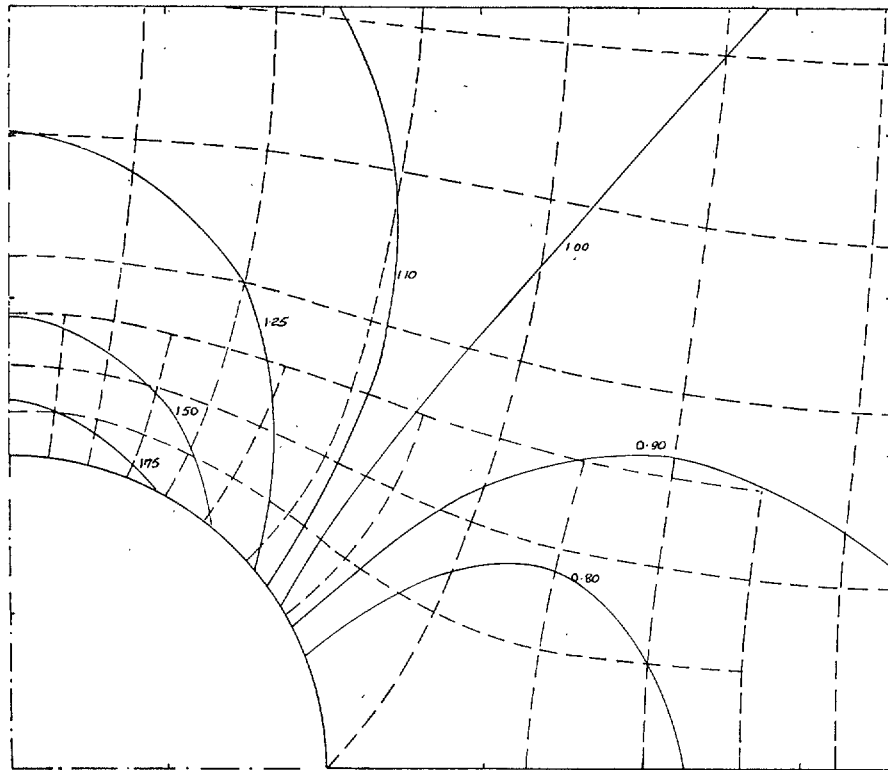


FIG. 9. Equi-velocity contours at  $M_0 = 0$ .

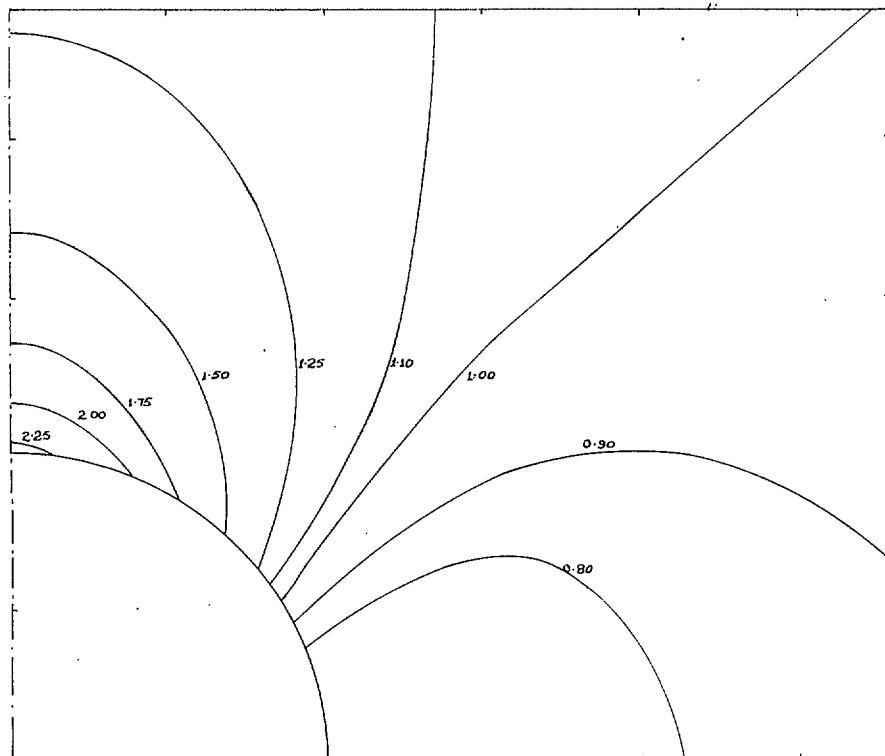


FIG. 10. Equi-velocity contours at  $M_0 = 0.35$ .

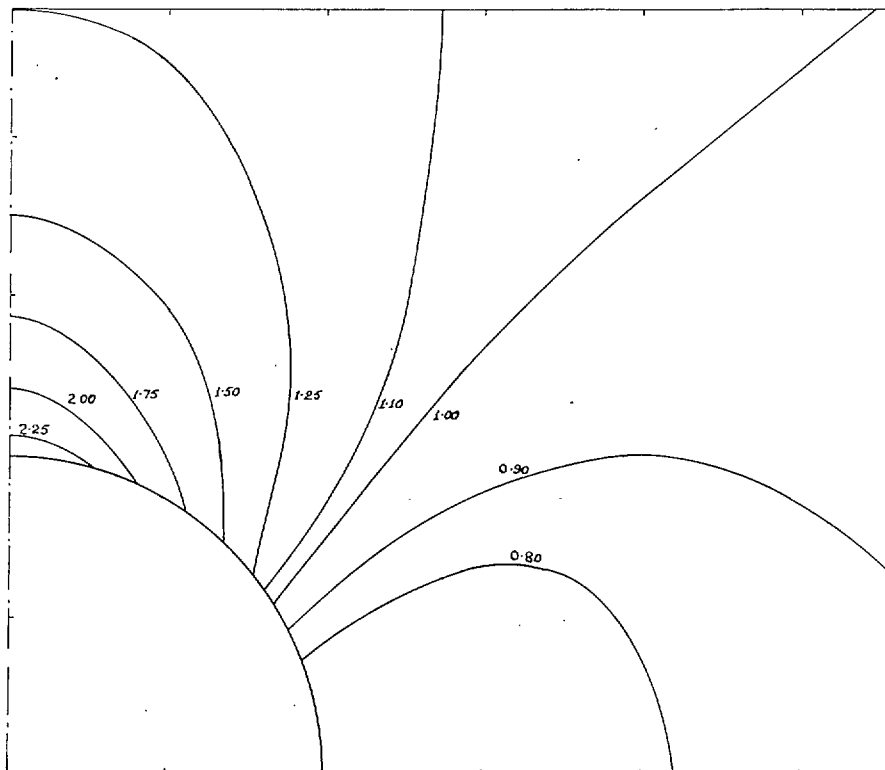


FIG. 11. Equi-velocity contours at  $M_0 = 0.40$ .

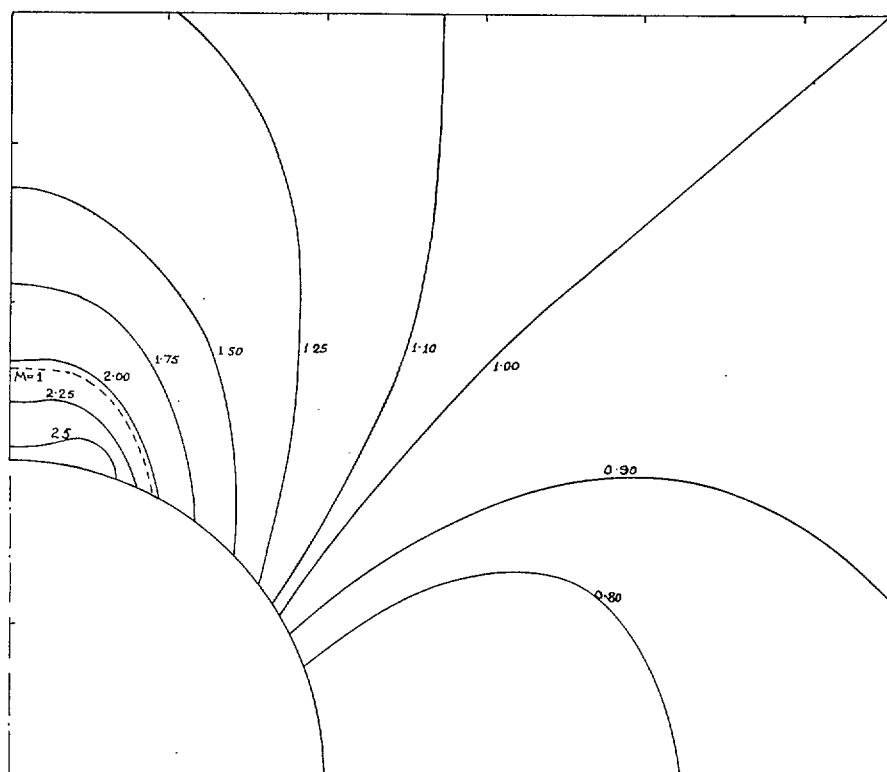


FIG. 12. Equi-velocity contours at  $M_0 = 0.45$ .

## Publications of the Aeronautical Research Council

### ANNUAL TECHNICAL REPORTS OF THE AERONAUTICAL RESEARCH COUNCIL (BOUND VOLUMES)

- 1936 Vol. I. Aerodynamics General, Performance, Airscrews, Flutter and Spinning. 40s. (40s. 9d.)  
Vol. II. Stability and Control, Structures, Seaplanes, Engines, etc. 50s. (50s. 10d.)
- 1937 Vol. I. Aerodynamics General, Performance, Airscrews, Flutter and Spinning. 40s. (40s. 10d.)  
Vol. II. Stability and Control, Structures, Seaplanes, Engines, etc. 60s. (61s.)
- 1938 Vol. I. Aerodynamics General, Performance, Airscrews. 50s. (51s.)  
Vol. II. Stability and Control, Flutter, Structures, Seaplanes, Wind Tunnels, Materials. 30s. (30s. 9d.)
- 1939 Vol. I. Aerodynamics General, Performance, Airscrews, Engines. 50s. (50s. 11d.)  
Vol. II. Stability and Control, Flutter and Vibration, Instruments, Structures, Seaplanes, etc.  
63s. (64s. 2d.)
- 1940 Aero and Hydrodynamics, Aerofoils, Airscrews, Engines, Flutter, Icing, Stability and Control,  
Structures, and a miscellaneous section. 50s. (51s.)
- 1941 Aero and Hydrodynamics, Aerofoils, Airscrews, Engines, Flutter, Stability and Control, Structures.  
63s. (64s. 2d.)
- 1942 Vol. I. Aero and Hydrodynamics, Aerofoils, Airscrews, Engines. 75s. (76s. 3d.)  
Vol. II. Noise, Parachutes, Stability and Control, Structures, Vibration, Wind Tunnels.  
47s. 6d. (48s. 5d.)
- 1943 Vol. I. (In the press.)  
Vol. II. (In the press.)

### ANNUAL REPORTS OF THE AERONAUTICAL RESEARCH COUNCIL—

1933-34	1s. 6d. (1s. 8d.)	1937	2s. (2s. 2d.)
1934-35	1s. 6d. (1s. 8d.)	1938	1s. 6d. (1s. 8d.)
April 1, 1935 to Dec. 31, 1936.	4s. (4s. 4d.)	1939-48	3s. (3s. 2d.)

### INDEX TO ALL REPORTS AND MEMORANDA PUBLISHED IN THE ANNUAL TECHNICAL REPORTS AND SEPARATELY—

April, 1950 - - - - R. & M. No. 2600. 2s. 6d. (2s. 7½d.)

### AUTHOR INDEX TO ALL REPORTS AND MEMORANDA OF THE AERONAUTICAL RESEARCH COUNCIL—

1909-1949 - - - - R. & M. No. 2570. 15s. (15s. 3d.)

### INDEXES TO THE TECHNICAL REPORTS OF THE AERONAUTICAL RESEARCH COUNCIL—

December 1, 1936—June 30, 1939.	R. & M. No. 1850.	1s. 3d. (1s. 4½d.)
July 1, 1939—June 30, 1945.	R. & M. No. 1950.	1s. (1s. 1½d.)
July 1, 1945—June 30, 1946.	R. & M. No. 2050.	1s. (1s. 1½d.)
July 1, 1946—December 31, 1946.	R. & M. No. 2150.	1s. 3d. (1s. 4½d.)
January 1, 1947—June 30, 1947.	R. & M. No. 2250.	1s. 3d. (1s. 4½d.)
July, 1951. - - - -	R. & M. No. 2350.	1s. 9d. (1s. 10½d.)

*Prices in brackets include postage.*

Obtainable from

### HER MAJESTY'S STATIONERY OFFICE

York House, Kingsway, London, W.C.2; 423 Oxford Street, London, W.1 (Post  
Orders: P.O. Box 569, London, S.E.1); 13a Castle Street, Edinburgh 2; 39 King Street,  
Manchester 2; 2 Edmund Street, Birmingham 3; 1 St. Andrew's Crescent, Cardiff;  
Tower Lane, Bristol 1; 80 Chichester Street, Belfast or through any bookseller.